Received: 18 September 2017 | Revised: 22 December 2017 | Accepted: 25 January 2018

DOI: 10.1002/mrm.27136

NOTE

Magnetic Resonance in Medicine

Simultaneous multislice acquisition without trajectory modification for hyperpolarized ^{13}C experiments

Angus Z. Lau[1,2] | Justin Y. C. Lau[1,2] | Albert P. Chen[3] | Charles H. Cunningham[1,2]

[1] Physical Sciences, Sunnybrook Research Institute, Toronto, Ontario, Canada

[2] Department of Medical Biophysics, University of Toronto, Toronto, Ontario, Canada

[3] GE Healthcare, Toronto, Ontario, Canada

Correspondence
Angus Z. Lau, Sunnybrook Research Institute, Room M7-600, Toronto, Ontario M4N 3M5, Canada.
Email: angus.lau@sri.utoronto.ca

Funding information
Natural Sciences and Engineering Research Council of Canada, Grant: RGPIN-2017-06596; Heart and Stroke Foundation of Canada, Grant: G-14-005743; Canadian Institutes of Health Research, Grant: MOP-133544

Purpose: To investigate the feasibility of performing large FOV hyperpolarized ^{13}C metabolic imaging using simultaneous multislice excitation.

Methods: A spectral-spatial multislice excitation pulse was constructed by cosine modulation and incorporated into a ^{13}C spiral imaging sequence. Phantom and in vivo pig experiments were performed to test the feasibility of simultaneous multislice data acquisition and image reconstruction. In vivo cardiac-gated images of hyperpolarized pyruvate, bicarbonate, and lactate were obtained at $1 \times 1 \times 1\,cm^3$ resolution over a $48 \times 48 \times 24\,cm^3$ FOV with 2-fold acceleration in the slice direction. Sensitivity encoding was used for image reconstruction with both autocalibrated and numerically calculated coil sensitivities.

Results: Simultaneous multislice images obtained with 2-fold acceleration were comparable to reference unaccelerated images. Retained SNR figures greater than 80% were achieved over the part of the image containing the heart.

Conclusion: This method is anticipated to enable large FOV imaging studies using hyperpolarized ^{13}C substrates, with an aim toward whole-body exams that have to date been out of reach.

KEYWORDS
^{13}C, hyperpolarization, parallel imaging, simultaneous multislice

1 | INTRODUCTION

Hyperpolarization of ^{13}C-enriched substrates using dissolution dynamic nuclear polarization has emerged as a promising tool for noninvasive, in vivo characterization of the metabolic state of tissues.[1] This technique results in transient signal enhancements relative to thermal equilibrium in excess of 10 000-fold, and has been used extensively to investigate metabolic alterations in preclinical models of cancer[2–5] and heart disease.[6,7] The feasibility of performing hyperpolarized MR measurements of metabolism in humans has also been shown recently.[8,9]

To date, most studies have focused on metabolic imaging of a single organ (e.g., heart, liver, brain, various tumor sites). However, disease processes often affect the body systemically, and metabolic alterations that occur in multiple organs or sites are often of clinical interest. For example, patients with type II diabetes exhibit an insensitivity to insulin, which drives systemic changes in pyruvate metabolism

Correction added after online publication 15 February. The authors have added funding information.

in both the heart and liver.[10] Assessment of metabolic changes over a large imaging volume could also be useful for identifying distant metastatic lesions, which are commonly characterized by increased uptake of 2-deoxy-2-[^{18}F] fluoro-D-glucose using whole-body PET/CT examinations.[11]

However, it still remains difficult to achieve volumetric whole-body coverage of multiple hyperpolarized ^{13}C labeled metabolites. This is because the total scan time is limited by both the relatively short lifetime of the hyperpolarized signal enhancement (approximately 60 seconds for [1-^{13}C]pyruvate at 3 T[12], and maximum feasible breath-hold durations (< 20 seconds). These limitations restrict the number of RF excitations that can be applied to produce ^{13}C images. Furthermore, ^{13}C RF transmit and receive coils, which cover the whole body, are not yet commercially available, but these physical limitations must be addressed first, and the development of whole-body ^{13}C imaging strategies can guide the development of ^{13}C array receivers.

Simultaneous multislice (SMS) acceleration is a promising method for achieving large FOV metabolic imaging using hyperpolarized ^{13}C MRI.[13–15] This method replaces the conventional single-slice RF pulse in a multislice acquisition with a multiband RF pulse, which selectively excites 2 or more spatial slices in a single TR. Signals from multiple slices are then separated using coil sensitivity information as input to parallel imaging reconstruction methods such as SENSE or GRAPPA.[16,17] Recently, we proposed combining SMS acceleration with spectral-spatial excitation of the desired ^{13}C metabolites of interest to improve spatial coverage.[18] Controlled aliasing by phase modulation of each slice during the readout improves conditioning of the inverse problem when the coil sensitivities between slices are not distinct. However, for single-shot k-space trajectories such as spiral or EPI, this requires gradient modulation along the slice-select direction.[15] Trajectory modification can be sensitive to gradient imperfections as a result of effects such as eddy currents, and may require accurate measurement of the k-space trajectory.[19–21] Another SMS approach was demonstrated for hyperpolarized ^{3}He spins. In this approach, gradients along the slice-select direction are used to rephase distinct linear phase profiles corresponding to each excited slice.[22] This trajectory modification is difficult to adapt for relatively long ^{13}C single-shot imaging trajectories (approximately 30 ms) because of potential T_2^*-related signal modulation between slices.

The aim of this study was to investigate the feasibility of performing large FOV hyperpolarized ^{13}C metabolic imaging using SMS excitation, without any additional trajectory modification. We demonstrate that the inherent coil sensitivity variations of a commercially available ^{13}C receiver coil array are sufficient to separate multiple excited slices, and show efficacy using phantom and in vivo experiments. Using SMS excitation, hyperpolarized [1-^{13}C]pyruvate, ^{13}C-bicarbonate, and [1-^{13}C] lactate can be imaged over a $48 \times 48 \times 24\,cm^3$ FOV with $1 \times 1 \times 1\,cm^3$ resolution in 24 heart beats. We anticipate that this method will become an important component of hyperpolarized ^{13}C imaging exams with extended coverage of the body.

2 | METHODS

2.1 | Excitation pulse design

A spectral-spatial excitation pulse (18 ms duration, 1 ms gradient sublobes, passband full width at half maximum 100 Hz, stopband width 1000 Hz) was designed to excite single spatial slices for individual resonances in a hyperpolarized [1-^{13}C]pyruvate spectrum, as previously described.[23,24] The peak B_1 required for a 60° excitation on the ^{13}C nucleus was 8.1 μT. The single-slice pulse was used for experiments determining the optimal configuration and orientation of the receive coil. A multiband pulse exciting 2 slices was produced by cosine modulation of the single-slice RF pulse using the gradient amplitude waveform. For experiments using the SMS pulse, the slice thickness was set to 1 cm with a center-to-center slice gap of 9 to 12 cm, depending on application. The peak B_1 required for a 60° 2-slice excitation scaled linearly to 16.2 μT. The RF waveform, gradient waveform, and spectral-spatial response are shown in Figure 1.

2.2 | Phantom experiments

A GE MR750 3T MRI (GE Healthcare, Waukesha, WI) with a clamshell ^{13}C volume transmit coil (GE Healthcare, Cleveland, OH) and ^{13}C 8-channel receive coil (2 rigid paddles, $20 \times 24\,cm^2$ each with 4 $5.5 \times 9.5\,cm^2$ elements oriented in a 1×4 array) was used for this study. The placement of the coil array is shown in Figure 2A.

The g-factor for 2-fold slice acceleration using the receive coil in different orientations was measured using a spherical phantom with 18-cm outer diameter containing ethylene glycol (99%, 0.36 M natural abundance ^{13}C). A spectrally selective, single-shot spiral sequence (TR = 5 seconds, FOV = 480 mm, readout duration = 32 ms, nominal in-plane resolution = $7.5 \times 7.5\,mm^2$, 8 slices, flip angle = 90°, number of excitations = 128) was used for imaging.[24] The slice thickness was set to 20 mm. As shown in Figure 2B, the scan was repeated twice with the receive coil placed such that the linear row of elements within the paddle was rotated 90° between scans. Thus, the elements were oriented either parallel with the imaging slices (along the major axis of the coil array), or perpendicular to the imaging slices (along the minor axis of the coil array). Fast spin-echo ^{1}H images were also acquired for reference, using the body coil for signal transmission and reception (TR = 486 ms, TE = 10.6 ms, FOV = 480 mm, in-plane resolution = $2.5 \times 2.5\,mm^2$, slice thickness = 2 mm).

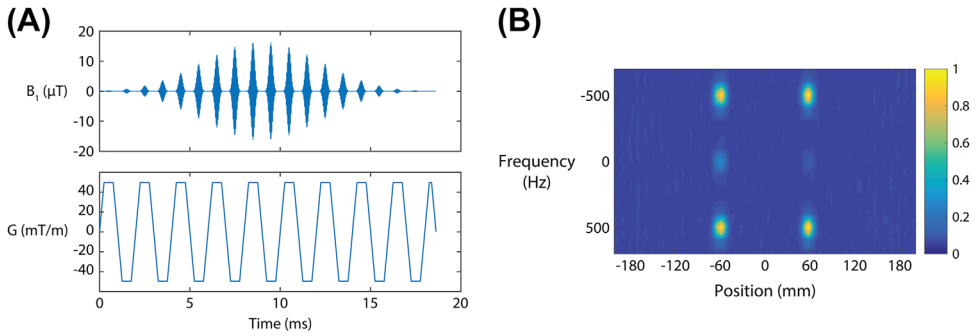

FIGURE 1 Spectral-spatial, multislice excitation pulse for accelerated hyperpolarized ^{13}C imaging. A, Radiofrequency and gradient waveforms. B, The measured spectral-spatial response shows the transverse magnetization (60 ° flip angle) in the 2 spatial positions excited by this pulse

In a second phantom experiment, the feasibility of multiband image reconstruction was determined. To provide image features, solid 0.5-inch-diameter high-density polyethylene rods (McMaster-Carr, Cleveland, OH) were placed in rectangular containers of dimensions $14 \times 14 \times 24\,cm^3$. The containers were filled with ethylene glycol and placed on their sides, with the receive coils placed with elements running lengthwise along the length of the containers. This coil placement provides higher coil count for improved SENSE reconstruction along the slice-encoding direction, but reduces sensitivity across the entire sample. An optimal coil would have high channel count on both sides of the object. The slice selective pulse was replaced with a multiband pulse exciting 2 slices, spaced 12 slice thicknesses apart (TR = 5 seconds, FOV = 480 mm, readout duration = 32 ms, in-plane resolution = $7.5 \times 7.5\,mm^2$, flip angle = 60 °, number of excitations = 256, 24 slices, slice thickness = 10 mm, slice gap = 0 mm). A total of 12 excitations were required to encode a 240-mm FOV along the slice-select dimension with 2-fold slice acceleration. A reference acquisition was also obtained using the single-slice pulse, requiring a total of 24 excitations to encode the same FOV.

2.3 | In vivo experiments

All animal experiments were carried out under a protocol approved by the institutional animal care and use committee. Animal preparation and handling procedures have been previously described.[24] For this feasibility study, a Yorkshire pig was scanned (weight = 25 kg, heart rate = 60 bpm). An intravenous catheter was placed in the ear vein for injection of hyperpolarized [1-^{13}C]pyruvate. An oral carbohydrate load (25 g glucose in 1 L, Life Brand, Toronto) was administered approximately 1 hour before the pyruvate injection, to raise cardiac pyruvate dehydrogenase activity. The animal was positioned supine and feet first within the volume transmit coil system.

A total of 500 mg of [1-^{13}C]pyruvic acid containing 15-mM AH111501 sodium salt was polarized using a GE SpinLAB polarizer for approximately 3 hours. The acid was neutralized with a stoichiometric quantity of a base solution (720-mM NaOH, 400-mM Trizma pH 7.6, 100 mg/L ethylenediaminetetraacetic acid) and diluted to a concentration of 250 mM. After dissolution, a volume of 20 mL of the 250-mM hyperpolarized [1-13C]pyruvate solution was injected at 4 mL/s, followed by a 25-mL saline flush at 5 mL/s.

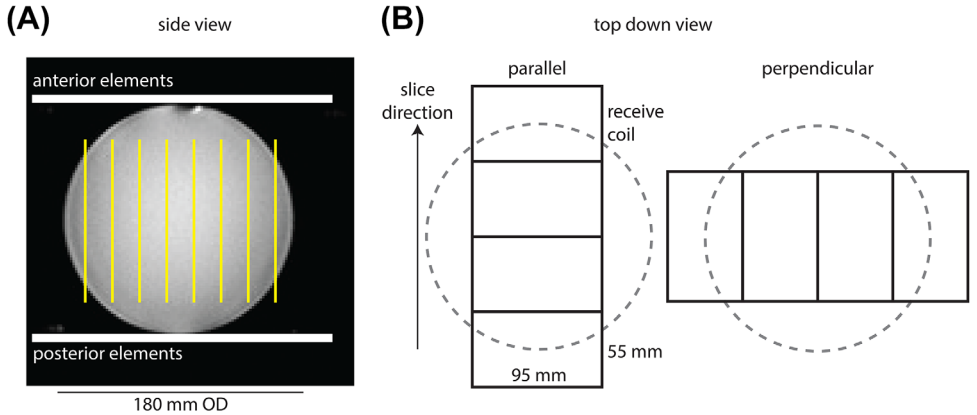

FIGURE 2 Experimental setup. A, Side view of a 180-mm outer-diameter sphere containing 0.36 M natural abundance ^{13}C ethylene glycol. The phantom is placed between 2 rigid paddles, each containing 4 receive elements in a 1×4 array. The axial ^{13}C slice orientation is indicated in yellow. B, The top-down view shows the linear row of coil elements oriented either parallel with or perpendicular to the axial stack of slices

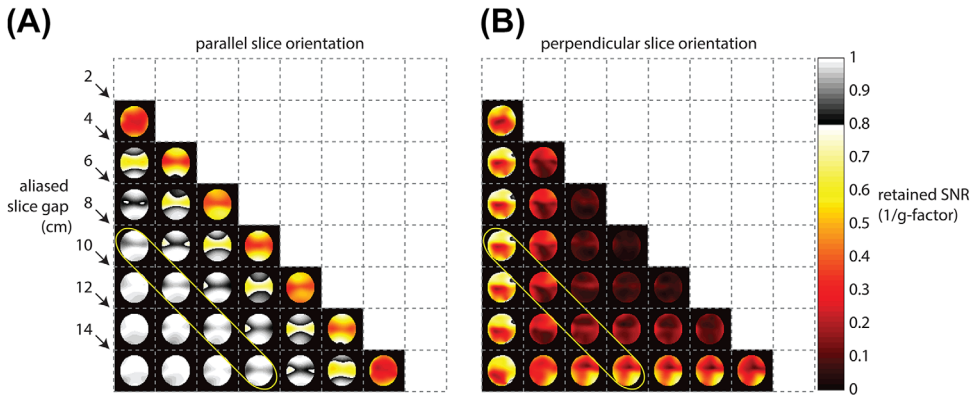

FIGURE 3 Retained SNR (1/g-factor) maps for the 8-channel receive array. A, Pairwise combinations of slices result in retained SNR maps that can be viewed as a 2D matrix. A higher retained SNR figure indicates better parallel imaging performance. The indicated diagonal band of elements corresponds to an 8-cm slice gap. Maps are cropped to a $24 \times 24\,cm^2$ FOV. B, Histogram of retained SNR values for the 8-cm slice gap shown. For the parallel slice orientation, retained SNR is greater than 80%

The single-shot spiral sequence was used in a spectrally selective manner to sequentially excite the resonances arising from [1-^{13}C]lactate, ^{13}C-bicarbonate, and [1-^{13}C]pyruvate (parameters: TR = 1 R-R interval, FOV = 480 mm, readout duration = 32 ms, nominal in-plane resolution = $7.5 \times 7.5\,mm^2$, 24 total slices, 3 excitations per heartbeat, slice thickness = 10 mm, gap = 0 mm, flip angle = 60° for all metabolites). The full 3D FOV was $48 \times 48 \times 24\,cm^3$. To test the effects of SMS excitation, 2 injections were performed, using either the single-slice pulse or the multiband pulse for RF excitation. The unaccelerated scan time to image the 3 resonances was 24 heartbeats. The 2-fold accelerated scan time was 12 heartbeats, and this was repeated 2 times to maintain a total breath-held scan time of 24 heartbeats. For a heart rate of 60 bpm, this corresponded to a total scan time of 24 seconds. The receive coils were placed on the chest wall, with the linear row of elements oriented parallel to the axial imaging slices. Fiducial markers visible on MRI (MR-SPOTS, Beekley Medical, Bristol, CT) were placed on the edges of the coil housing for each paddle. The scan started 20 seconds after the start of the injection to maximize the ^{13}C-bicarbonate signal in the myocardium.[24] Axial, cardiac-gated breath-held SSFP cine ^{1}H images were acquired for anatomical reference (TR = 4.2 ms, TE = 1.8 ms, FOV = 240 mm, slice thickness = 5 mm, matrix size = 224×224).

2.4 | Coil sensitivity estimation

Images were reconstructed by NUFFT using the Berkeley Advanced Reconstruction Toolbox (https://mrirecon.github.io/bart/).[25] For phantom experiments, the ESPIRiT method was used to estimate coil sensitivities from low-resolution images.[26] For in vivo experiments, a low-resolution reference scan would require using nonrecoverable magnetization; thus, numerical high-resolution coil sensitivity estimates were calculated using the Biot-Savart law using fiducial marker positioning as previously described.[27]

2.5 | G-factor calculation

G-factor maps for 2-fold slice acceleration were computed using

$$g_i = \sqrt{(S^H S)^{-1}_{i,i} (S^H S)_{i,i}}, \quad (1)$$

where $i = 1,2$ and S is an $N_{coil} \times N_{slice}$ sensitivity matrix. The retained SNR (1/g) is reported. Pairwise g-factor maps were computed for each combination of summed slices. The mutual noise resistance matrix was ignored in our analysis; this is a reasonable approximation at the 32-MHz ^{13}C frequency at 3 T.[27,28] A noise correlation matrix plot is included in Supporting Information Figure S3.

2.6 | Image reconstruction

Time domain signals were apodized using 10 Hz, resulting in a reconstructed image resolution of $1 \times 1 \times 1\,cm^3$. The SENSE matrix inversion was used to separate the 2-fold undersampling. Reference images for comparison were obtained using a single-slice excitation pulse. For the in vivo experiment, intensity correction was applied to pyruvate, bicarbonate, and lactate images using the numerical coil sensitivities to remove apparent differences in bicarbonate signal intensity between the anterior and posterior myocardium.[27]

3 | RESULTS

Coil sensitivities were obtained in the ethylene glycol phantom. Distinct coil sensitivity variations (Supporting Information Figure S1) between slices were created by placing the paddles in different orientations relative to the imaging

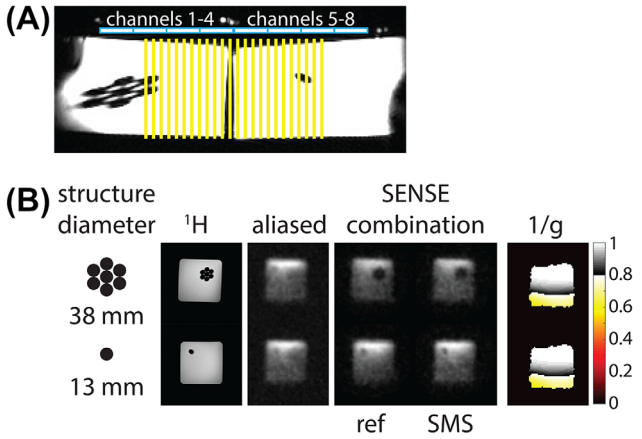

FIGURE 4 Simultaneous multislice (SMS) reconstructions of the ^{13}C ethylene glycol phantom. A, Experimental setup and side view of 2 rectangular containers filled with ^{13}C ethylene glycol. The linear row of coil elements run along the side of the phantom; the yellow lines indicate 24 axial slices. B, Reconstructed images in 2 slices are shown. The images are cropped to a 24 × 24 cm^2 FOV

slices. To characterize the performance using different coil orientations, Figure 3 shows retained SNR (1/g-factor) maps for pairwise combination of slices, corresponding to 2-fold acceleration. For 2-fold acceleration, this can be represented as a 2D triangular matrix, in which diagonal matrix elements indicate a constant slice gap. The maps demonstrate improved conditioning of the parallel imaging reconstruction, depending on coil orientation. The color scale is such that grayscale indicates a retained SNR greater than 80%. Figure 3B shows a retained SNR histogram for all slice combinations with 8-cm slice gap, which indicates that in the parallel coil configuration, the retained SNR is greater than 80%.

A comparison between single-band ("ref") and multiband ("SMS") excitation in the ethylene glycol phantom is shown in Figure 4. The high-density polyethylene rods are well resolved in the multiband scan, and the retained SNR map indicates good performance over the region near the receive coils.

Figure 5 shows 2 slices from the in vivo scan of hyperpolarized [1-^{13}C]pyruvate and its downstream metabolites, lactate and bicarbonate. These slices are separated by 12 cm, and the 2 time points for the SMS accelerated scan are shown for both pyruvate and bicarbonate. Retained SNR maps computed using 2-fold undersampling with the numerically estimated coil sensitivities show good performance (greater than 80% of retained SNR) over the part of the image containing the heart.

4 | DISCUSSION

The ^{13}C coil configuration (volume transmit with anterior–posterior receive array) has recently been used to image human cardiac metabolism.[9] This study shows that the setup

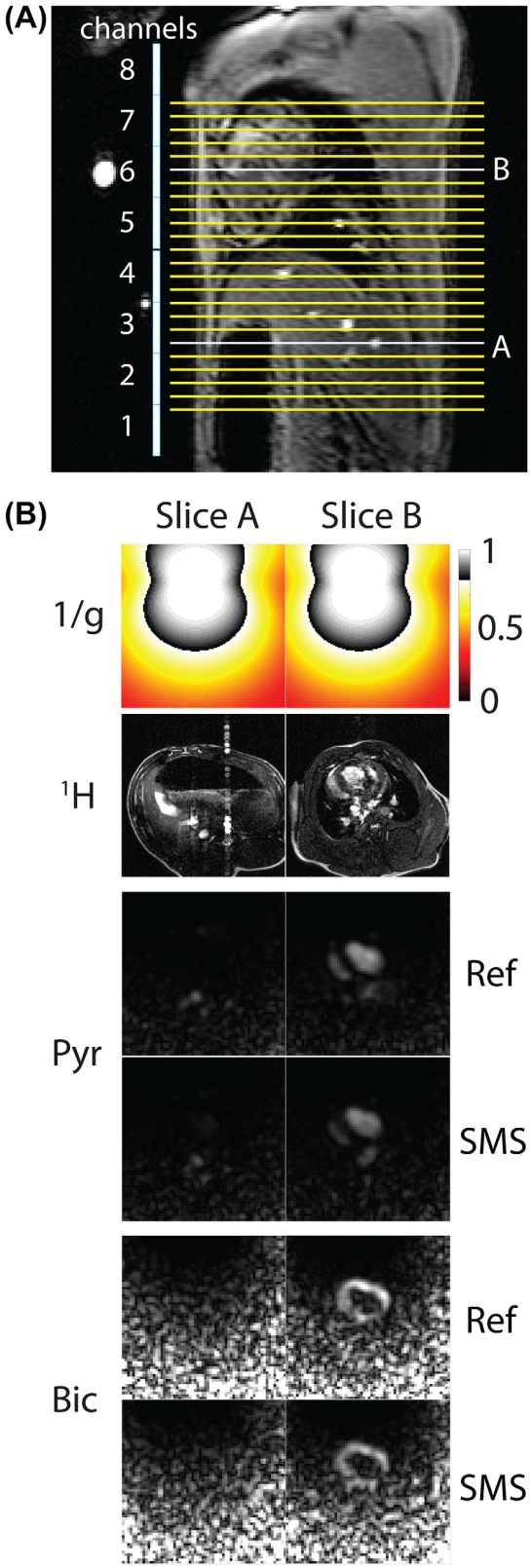

FIGURE 5 Simultaneous multislice reconstructions of hyperpolarized ^{13}C pyruvate and bicarbonate in vivo. A, Sagittal localizer showing array elements and slice positions relative to the anatomy. B, Numerical Biot-Savart coil sensitivities were used for uniform image reconstruction. Retained SNR (1/g) maps show noise amplification in the posterior anatomy. Images are cropped to a 24 × 24 cm^2 FOV

can be easily adapted to accelerate existing clinical ^{13}C imaging methods. This approach is feasible as long as care is taken to orient the imaging slices parallel to the individual coil elements. Even larger FOVs could be achieved by placing multiple paddles along the anterior chest wall. Increasingly larger FOVs are eventually limited by the B_1 inhomogeneity of the ^{13}C volume transmit coil. A ^{13}C body coil could improve B_1 homogeneity and potentially allow for true whole-body imaging.

This development will potentially enable whole-body, large FOV imaging of multiple organs (e.g., heart, liver, brain), especially as extended high channel count ^{13}C receiver arrays become available. Such receiver arrays are especially suited for ^{13}C imaging. Distant elements can be easily decoupled, and given the relatively high cost of the HP ^{13}C probe, it is reasonable to maximize the amount of information acquired per injection to help us better understand the potentials and limitations of this method.

In this study, we aimed to demonstrate the feasibility of SMS acceleration using a protocol that is already being clinically used to study human cardiac metabolism. Dynamic acquisition would be useful for modeling the conversion of pyruvate into its downstream metabolites. We previously demonstrated that dynamic cardiac imaging in pigs is possible, with the sampling of 3 metabolic volumes at 7.5-second temporal resolution.[29] With SMS acceleration, it would be possible to acquire free-breathing, dynamic metabolic volumes of the whole body with the same temporal resolution, by increasing the number of slices imaged per R-R interval.

For hyperpolarized magnetization, the benefits of time-averaging to improve image SNR are largely eliminated, as the total signal is nonrecoverable. Thus, it is favorable to image as quickly as possible. Simultaneous multislice affects SNR via g-factor noise penalty only ($SNR_{SMS} = SNR/g$) without a corresponding scan-time reduction penalty.

By imaging slices spaced far apart, we circumvent the need for additional gradient blips in the through-slice direction. Gradient blips applied during a single-shot readout are sensitive to gradient timing errors and can lead to image artifacts that are difficult to correct. Interslice phase modulation may also be incompatible with thick slices, which can violate the controlled aliasing assumption of unique phases per simultaneously acquired slice.[30] Thinner slice excitation would allow gradient modulation to be used, which could be important for allowing slice gaps less than 8 cm, as used in this study. This would need to be carefully balanced with the SNR reduction from the thin slices.

An important consideration is whether off-resonance excitation affects the SMS reconstruction. Given typical whole-heart linewidths obtained using automated shimming with this setup (approximately 1 ppm), images reconstructed using a single frequency did not result in noticeable resolution differences between slices. If this was not the case, the SENSE reconstruction would need to be modified to account for varying spatial off-resonance frequencies to avoid slice-dependent blurring artifacts.

For the in vivo experiments, numerically estimated coil sensitivities were used for SMS image reconstruction. As the magnetization is nonrecoverable, this avoids the need to acquire a low-resolution reference scan, as is commonly done in ^{1}H imaging. Figure 5 shows that numerically estimated coil sensitivities can be used for SMS image reconstruction. The noise increases posteriorly as a result of the intensity correction used to compensate for the anterior chest wall coil array position. This effect could be reduced by scanning with paddles placed on the posterior wall at the expense of superior–inferior coverage.

5 | CONCLUSIONS

Simultaneous multislice imaging was explored as a method to accelerate hyperpolarized ^{13}C imaging experiments. Spectral-spatial multislice excitation was used to obtain images of hyperpolarized [1-^{13}C]pyruvate, ^{13}C-bicarbonate, and [1-^{13}C]lactate over a $48 \times 48 \times 24\,cm^3$ FOV. This method is anticipated to facilitate large FOV imaging studies using hyperpolarized ^{13}C substrates, with an aim toward whole-body exams that have to date been out of reach.

REFERENCES

[1] Ardenkjaer-Larsen JH, Fridlund B, Gram A, et al. Increase in signal-to-noise ratio of > 10,000 times in liquid-state NMR. *Proc Natl Acad Sci U S A.* 2003;100:10158-10163.

[2] Day SE, Kettunen MI, Gallagher FA, et al. Detecting tumor response to treatment using hyperpolarized 13C magnetic resonance imaging and spectroscopy. *Nat Med.* 2007;13:1382-1387.

[3] Golman K, Zandt RI, Lerche M, Pehrson R, Ardenkjaer-Larsen JH. Metabolic imaging by hyperpolarized 13C magnetic resonance imaging for in vivo tumor diagnosis. *Cancer Res.* 2006; 66:10855-10860.

[4] Albers MJ, Bok R, Chen AP, et al. Hyperpolarized 13C lactate, pyruvate, and alanine: noninvasive biomarkers for prostate cancer detection and grading. *Cancer Res.* 2008;68:8607-8615.

[5] Chen AP, Albers MJ, Cunningham CH, et al. Hyperpolarized C-13 spectroscopic imaging of the TRAMP mouse at 3T-initial experience. *Magn Reson Med.* 2007;58:1099-1106.

[6] Schroeder MA, Cochlin LE, Heather LC, Clarke K, Radda GK, Tyler DJ. In vivo assessment of pyruvate dehydrogenase flux in the heart using hyperpolarized carbon-13 magnetic resonance. *Proc Natl Acad Sci U S A.* 2008;105:12051-12056.

[7] Schroeder MA, Lau AZ, Chen AP, et al. Hyperpolarized (13)C magnetic resonance reveals early- and late-onset changes to in

vivo pyruvate metabolism in the failing heart. *Eur J Heart Failure.* 2013;15:130-140.

[8] Nelson SJ, Kurhanewicz J, Vigneron DB, et al. Metabolic imaging of patients with prostate cancer using hyperpolarized [1-(1)(3)C]pyruvate. *Sci Transl Med.* 2013;5:198ra108.

[9] Cunningham CH, Lau JY, Chen AP, et al. Hyperpolarized 13C metabolic MRI of the human heart: initial experience. *Circ Res.* 2016;119:1177-1182.

[10] Le Page LM, Ball DR, Ball V, et al. Simultaneous in vivo assessment of cardiac and hepatic metabolism in the diabetic rat using hyperpolarized MRS. *NMR Biomed.* 2016;29:1759-1767.

[11] Gambhir SS. Molecular imaging of cancer with positron emission tomography. *Nat Rev Cancer.* 2002;2:683-693.

[12] Golman K, in 't Zandt R, Thaning M. Real-time metabolic imaging. *Proc Natl Acad Sci U S A.* 2006;103:11270-11275.

[13] Larkman DJ, Hajnal JV, Herlihy AH, Coutts GA, Young IR, Ehnholm G. Use of multicoil arrays for separation of signal from multiple slices simultaneously excited. *J Magn Reson Imaging.* 2001;13:313-317.

[14] Breuer FA, Blaimer M, Heidemann RM, Mueller MF, Griswold MA, Jakob PM. Controlled aliasing in parallel imaging results in higher acceleration (CAIPIRINHA) for multi-slice imaging. *Magn Reson Med.* 2005;53:684-691.

[15] Setsompop K, Gagoski BA, Polimeni JR, Witzel T, Wedeen VJ, Wald LL. Blipped-controlled aliasing in parallel imaging for simultaneous multislice echo planar imaging with reduced g-factor penalty. *Magn Reson Med.* 2012;67:1210-1224.

[16] Pruessmann KP, Weiger M, Scheidegger MB, Boesiger P. SENSE: sensitivity encoding for fast MRI. *Magn Reson Med.* 1999;42:952-962.

[17] Griswold MA, Jakob PM, Heidemann RM, et al. Generalized autocalibrating partially parallel acquisitions (GRAPPA). *Magn Reson Med.* 2002;47:1202-1210.

[18] Lau AZ, Dominguez-Viqueira W, Cunningham CH, Robson MD, Tyler DJ. Simultaneous multi-slice imaging of multiple metabolites using spectral-spatial excitation for hyperpolarized 13C experiments. In: Proceedings of the 22nd Annual Meeting of ISMRM, Milan, Italy, 2014. p. 981.

[19] Duyn JH, Yang Y, Frank JA, van der Veen JW. Simple correction method for k-space trajectory deviations in MRI. *J Magn Reson.* 1998;132:150-153.

[20] Vannesjo SJ, Haeberlin M, Kasper L, et al. Gradient system characterization by impulse response measurements with a dynamic field camera. *Magn Reson Med.* 2013;69:583-593.

[21] Addy NO, Wu HH, Nishimura DG. Simple method for MR gradient system characterization and k-space trajectory estimation. *Magn Reson Med* 2012;68:120-129.

[22] Teh K, Lee KJ, Paley MN, Wild JM. Parallel imaging of hyperpolarized helium-3 with simultaneous slice excitation. *Magn Reson Med.* 2006;55:258-262.

[23] Cunningham CH, Chen AP, Lustig M, et al. Pulse sequence for dynamic volumetric imaging of hyperpolarized metabolic products. *J Magn Reson.* 2008;193:139-146.

[24] Lau AZ, Chen AP, Ghugre NR, et al. Rapid multislice imaging of hyperpolarized 13C pyruvate and bicarbonate in the heart. *Magn Reson Med.* 2010;64:1323-1331.

[25] Tamir JI OF, Cheng JY, Uecker M, Lustig M. Generalized magnetic resonance image reconstruction using the Berkeley Advanced Reconstruction Toolbox. In: Proceedings of the ISMRM Workshop on Data Sampling and Image Reconstruction, Sedona, AZ, 2016.

[26] Uecker M, Lai P, Murphy MJ, et al. ESPIRiT—an eigenvalue approach to autocalibrating parallel MRI: where SENSE meets GRAPPA. *Magn Reson Med.* 2014;71:990-1001.

[27] Dominguez-Viqueira W, Geraghty BJ, Lau JY, Robb FJ, Chen AP, Cunningham CH. Intensity correction for multichannel hyperpolarized 13C imaging of the heart. *Magn Reson Med.* 2016;75:859-865.

[28] Roemer PB, Edelstein WA, Hayes CE, Souza SP, Mueller OM. The NMR phased array. *Magn Reson Med.* 1990;16:192-225.

[29] Lau AZ, Chen AP, Barry J, et al. Reproducibility study for free-breathing measurements of pyruvate metabolism using hyperpolarized (13) C in the heart. *Magn Reson Med.* 2013;69:1063-1071.

[30] Lau AZ, Tunnicliffe EM, Frost R, Koopmans PJ, Tyler DJ, Robson MD. Accelerated human cardiac diffusion tensor imaging using simultaneous multislice imaging. *Magn Reson Med.* 2015;73:995-1004.

SUPPORTING INFORMATION

Additional Supporting Information may be found in the supporting information tab for this article.

FIGURE S1 Low-resolution coil sensitivity maps for the 8-channel receive array with the ethylene glycol phantom. The paddles were placed with the elements oriented either parallel (left), or perpendicular (right), to the prescribed imaging slices. Maps are cropped to a $24 \times 24\,cm^2$ FOV

FIGURE S2 Simultaneous multislice reconstructions of hyperpolarized ^{13}C pyruvate, lactate, and bicarbonate in vivo. Below the proton reference, the first group of images shows the SMS reconstruction, and the second group of images shows the reference images. Columns represent different slices. Images are cropped to a $12 \times 12\,cm^2$ FOV

FIGURE S3 Noise correlation matrix plot for the ^{13}C receive coil. Noise was taken from a dummy scan performed prior to the ^{13}C injection. This result shows that the channels are well decoupled, and implies that the noise matrix can be well approximated by the identity matrix

How to cite this article: Lau AZ, Lau JYC, Chen AP, Cunningham CH. Simultaneous multislice acquisition without trajectory modification for hyperpolarized ^{13}C experiments. *Magn Reson Med.* 2018;80:1588–1594. https://doi.org/10.1002/mrm.27136